Available online at www.sciencedirect.com
SCIENCE DIRECT®
PERGAMON
Deep-Sea Research I 49 (2002) 2163–2181
DEEP-SEA RESEARCH PART I
www.elsevier.com/locate/dsr

High concentrations of exopolymeric substances in Arctic winter sea ice: implications for the polar ocean carbon cycle and cryoprotection of diatoms

C. Krembs[a,*], H. Eicken[b], K. Junge[a], J.W. Deming[a]

[a] *School of Oceanography, University of Washington, P.O. Box 357940, Seattle, WA, USA*
[b] *Geophysical Institute, University of Alaska, Fairbanks, USA*

Received 8 January 2002; received in revised form 17 May 2002; accepted 17 September 2002

Abstract

Exopolymeric substances (EPS) produced by microorganisms play important roles in various aquatic, porous, and extreme environments. Only recently has their occurrence in sea ice been considered. We used macroscopic and microscopic approaches to study the content and possible ecological role of EPS in wintertime fast ice near Barrow, Alaska (71°20′ N, 156°40′ W). Using Alcian blue staining of melted ice samples, we observed high concentrations of EPS in all samples examined, ranging from 0.79 to 7.71 mg xanthan gum equivalents (XGEQV) l^{-1}. Areal conversions to carbon equivalents yielded 1.5–1.9 g C m^{-2} ice in March and 3.3–4.0 g C m^{-2} in May (when the ice was thicker). Although EPS did not correlate with macronutrient or pigment data, the latter analyses indicated ongoing or recent biological activity in the ice within temperature horizons of −11°C to −9°C and warmer. EPS correlated positively with bacterial abundance (although no functional relationship could be deduced) and with dissolved organic carbon (DOC) concentrations. Ratios of EPS/DOC decreased at colder temperatures within the core, arguing against physical conversion of DOC to EPS during freezing. When sea-ice segments were maintained at representative winter temperatures (−5°C, −15°C and −25°C) for 3–14 months, the total EPS content increased significantly at rates of 5–47 μg XGEQV l^{-1} d^{-1}, similar to published rates of EPS production by diatoms. Microscopic images of ice-core sections at these very cold temperatures, using a recently developed non-invasive method, revealed diatoms sequestered in spacious brine pockets, intact autofluorescent chloroplasts in 47% of the (pennate) diatoms observed, and indications of mucus in diatom-containing pores. The high concentrations of EPS detected in these winter ice cores represent a previously unrecognized form of organic matter that may contribute significantly to polar ocean carbon cycles, not only within the ice but after springtime release into the water column. The EPS present in very high concentrations in the brine of these microhabitats appear to play important buffering and cryoprotectant roles for microorganisms, especially diatoms, against harsh winter conditions of high salinity and potential ice-crystal damage.

Keywords: Arctic; Sea ice; Polysaccharides; Exopolymers; Diatom; Carbon

*Corresponding author.
E-mail address: ckrembs@ocean.washington.edu (C. Krembs).

0967-0637/03/$ - see front matter
PII: S0967-0637(02)00122-X

1. Introduction

With an average areal extent of $3.4 \times 10^6\,km^2$ (Maykut, 1985), sea ice provides a vast low-temperature habitat for many organisms, including a broad range of species of bacteria, fungi, algae, protozoa and metazoa (e.g., Horner et al., 1992). These organisms can persist at extremes of known physiological tolerance of temperature and salinity (e.g., Aletsee and Jahnke, 1992), yet their survival mechanisms in the winter months are not well understood. While reports on the physiological limits of temperature and salinity of sea-ice organisms are increasing (e.g., Kottmeier and Sullivan, 1990; Helmke and Weyland, 1995; Stoecker et al., 1997; Junge et al., 2001b), little is known about the spatial constraints that sea ice imposes during winter or the scope of mechanisms utilized by microorganisms to persist in a structurally changing ice habitat and perhaps even alter it to their advantage.

The sea-ice crystal matrix is permeated by a highly connected network of pores and brine channels, typically ranging between >1 and $<20\%$ volume as a result of temperature, salt content and ionic composition (Weeks and Ackley, 1986). As the ice cools during winter, the volume fraction of liquid decreases and the salinity of the brine increases in accordance with the thermodynamic phase equilibria governing the thermal evolution of the ice–brine system (Cox and Weeks, 1983; Marion and Grant, 1994). Thus, winter sea ice at $-15^\circ C$ to $-20^\circ C$ typically contains more than 1% volume filled with liquid brine of a salinity above 200. Brine inclusions, in general, range from several micrometers to centimeters in size and become increasingly disconnected at lower temperatures (Weissenberger et al., 1992; Golden et al., 1998; Freitag, 1999; Eicken et al., 2000).

Most of the biomass in Arctic sea ice is located in the lowermost centimeter-thick horizon where favorable conditions in proximity to the water allow an ice-associated (sympagic) community to develop (e.g., Horner et al., 1992). During ice growth, slow-moving or non-motile organisms become encased by ice and subsequently (during winter) experience decreases in temperature and habitable space and increases in salinity in the remaining brine. Intracellular adaptations to such conditions have been studied from a physiological and molecular perspective (e.g., Hargens and Shabica, 1973; Murase, 1992; Knight and DeVries, 1994; Kirst and Wiencke, 1995; Kawahara et al., 1996). The drastic changes that occur in sea ice, however, also beg the question of whether organisms may have extracellular means to alter and ameliorate their environment. Recently, viable organisms were found in sea ice at lower temperatures and higher salinities than previously reported (e.g., Helmke and Weyland, 1995; Stoecker et al., 1997; Junge et al., 2001b). The pennate diatom *Nitzschia frigida*, a typical Arctic ice alga (e.g., Syvertsen, 1991), grew at temperatures as low as $-8^\circ C$ (Aletsee and Jahnke, 1992) and corresponding salinity of 109. This work was especially insightful in describing high concentrations of mucus as a possible response to the harsh environmental conditions (Aletsee and Jahnke, 1992). Under nutrient limitation and even during absence of light, many benthic pennate diatoms are known to exude high amounts of exopolymeric substances (EPS; Smith et al., 1998; Smith and Underwood, 2000). Experiments simulating winter conditions in the dark have shown persistent activity in polar sea-ice and marine diatoms (Palmisano and Sullivan, 1985; Zhang et al., 1998). Several diatom species (e.g., McConville, 1985; Riebesell et al., 1991; Hoagland et al., 1993; McConville et al., 1999) and many bacteria (Okutani, 1985; Heissenberger and Herndl, 1994; Cooksey and Wigglesworth-Cooksey, 1995; Costerton et al., 1995; Stoderegger and Herndl, 1998; Deming and Baross, 2001) can produce copious quantities of EPS which accumulate as thick gels around the cells.

EPS consists mainly of acid mucopolysaccharides containing uronic acid (McConville, 1985). They belong partly (operationally) to the dissolved organic material and the colloidal and particulate gel size fractions (Alldredge and Crocker, 1995; Chin et al., 1998). The ecological significance of EPS as substances used by microbes to form and maintain protective microhabitats has been demonstrated for several aquatic systems (e.g., Decho, 1990, 2000), though not yet for sea ice. Although earliest observations of mucus scum and

brownish mucus slime associated with Arctic sea ice date back more than 150 years (Horner, 1996), sea ice has been largely overlooked as a potential carrier of carbon in the form of EPS (McConville, 1985; Gosselin et al., 1997; McConville et al., 1999; Krembs and Engel, 2001; Thomas et al., 2001).

Beginning in late winter of 1999, we collected first-year sea ice from the coastal fast ice of the Chukchi Sea near Point Barrow, Alaska, to determine the magnitude of EPS content and potential ecological consequences at temperatures colder than previously examined. We considered the seasonal persistence of EPS within the ice, its possible production under wintertime conditions, and its significance to sea-ice diatoms overwintering in the ice. In a three-pronged approach to these issues, we measured key biotic and abiotic parameters at near in situ conditions on samples collected in the field, incubated ice-core segments at subzero temperatures over long periods of time, and examined diatoms microscopically in their natural microhabitats at simulated in situ temperatures. We also related EPS content in the ice to concentrations of macronutrients, chlorophyll *a* (Chl *a*), bacteria, dissolved organic carbon (DOC) and sea-ice pore structure.

2. Material and methods

2.1. Sampling and field-related measurements

Cores of typical first-year Arctic sea ice (Eicken et al., 2000) were obtained with a 10-cm ice corer (powered by a portable generator and electric drill) from the coastal fast-ice cover of the eastern Chukchi Sea near Barrow, Alaska (71°20′N, 156°40′W) 50 m off the coast at a water depth of about 10 m. The first and most intensively analyzed cores were collected in early March, the coldest period of the winter of 1999. Additional cores were collected opportunistically 2 months later, on May 3, and after a new season of ice had formed in the fall, on November 4.

Vertical profiles of ice-core temperatures were measured directly in the field, immediately after coring, by drilling holes 5 cm deep at 5–10-cm intervals and inserting a temperature probe (Control Company, accuracy 0.2°C). Cores were then sleeved in plastic and placed in an insulated container that maintained the samples at near in situ temperatures (Eicken et al., 2000) during the short transport to the Ukpeagvik Inupiat Corporation-Naval Arctic Research Laboratory (UIC-NARL) in Barrow. In March, samples were processed on the day of collection at UIC-NARL to determine bulk salinity and Chl *a*, as described below. All other variables were analyzed at the Geophysical Institute, University of Alaska, Fairbanks (UAF), after transport and 1 week of storage at −15°C. The May and November ice cores were transferred directly to UAF and stored in the dark at −25°C (May core) and −20°C (±2°C; November core) until processing in August and December of 1999, respectively.

Bulk parameters of the ice cores were measured on 5- (salinity) or 10-cm (all other parameters) core segments that were melted in the dark. Salinity of the resulting meltwater was measured with a Yellow Springs Instruments (YSI) Model 30 conductivity sonde (measurement error $<0.02\%$ or $<1\%$ of the bulk salinity). To determine EPS content, 200 ml of the meltwater samples were filtered carefully onto 0.4-μm membrane filters (Nuclepore), supported by Whatman glass fiber (GF/F) filters, with a portable syringe system at a vacuum pressure below 0.1 bar. Filters were stained with a pre-filtered (0.2 μm) Alcian blue solution (Passow and Alldredge, 1995) for 1 min and then rinsed with distilled water. The stained filters were transferred into 6 ml of 80% sulfuric acid, held for 12 h to dissolve the stain, and centrifuged. The concentration of stained EPS was measured spectrophotometrically at 878 nm (UV/Vis Perkin Elmer spectrometer Lambda2S) by the colorimetric method of Passow and Alldredge (1995), which specifies the concentration of stained acid mucopolysaccharides in terms of xanthan gum equivalents (XGEQV). EPS concentrations were also converted from XGEQV to carbon, by the conversion factor of 0.75 (Engel and Passow, 2001), for comparison to DOC concentrations and other carbon estimates in the literature.

Macro-nutrient and pigment analyses were performed on the March ice samples to determine bulk concentrations. Volumes of 50 ml of the

meltwater samples were filtered through GF/F filters and stored at −80°C until analysis at the School of Oceanography, University of Washington, where UNESCO protocols (UNESCO, 1994) were used to determine levels of PO_4 and the dissolved inorganic nitrogen (DIN) species, NO_3, NO_2 and NH_4. Chl *a* and phaeophytin were measured by filtering 300–500 ml samples of the meltwater onto GF/F filters until they appeared colored. Filters were stored at −20°C in the dark for 1 month followed by extraction in 90% acetone at 0°C and analysis with a Turner fluorometer (Evans et al., 1987). Reliable pigment data were not obtained (or attempted) for the stored May (or November) ice samples because of unsuitable storage conditions.

Bacterial abundance in the meltwater was determined with the DNA-specific stain DAPI (4′,6′-diamidino-2-phenylindole 2HCl) and epifluorescence microscopy. Five-milliliters of subsamples were preserved with pre-filtered (0.2 μm) formaldehyde (2% final concentration), filtered onto 0.2 μm Nuclepore filters, overlain with 2 ml of the DAPI solution (20 μg ml^{-1}) and allowed to stain for 5 min. The filter was then mounted on a microscopic slide. Bacteria were counted on 20 randomly selected fields on the filter by epifluorescence microscopy at 1563× magnification (Porter and Feig, 1980).

For DOC analysis, three ice segments from a March core (0–10, 10–20, and 95–115 cm below surface) and 10-cm segments throughout a May core were deep-frozen from −25°C to −80°C 1 week prior to processing. Each segment was then split into several pieces. The outer portions of these ice fragments were rinsed (melted away) quickly with room-temperature distilled water to remove potential contaminating traces of organic carbon. The remaining pieces were then melted in muffled glass beakers covered with aluminum foil at room temperature. Volumes of 6-ml samples were pre-filtered through muffled GF/F filters to remove POC > 0.7 μm. DOC concentrations in the filtrates were measured after acidification with HCl by the high-temperature catalytic oxidation method with a Shimadzu TOC analyzer. POC was analyzed with a Leeman Labs Model CEC440 elemental analyzer.

To reconstruct the in situ concentrations of EPS, DOC and bacteria in the volume of brine held by the ice under in situ conditions, we followed the semi-empirical approach of Cox and Weeks (1983) using our measurements of ice-core temperatures in the field and bulk salinities in the laboratory. We thus assumed that organic molecules and bacteria were concentrated during the freezing process in a way similar to salts (e.g., Bronstein et al., 1981; Hung et al., 1996; Giannelli et al., 2001). Specifically, in situ concentrations in the brine were calculated by dividing the respective concentrations of EPS, DOC or bacteria in the bulk ice (meltwater) by the relative brine volume fraction at a given temperature.

2.2. Long-term incubation of ice-core segments

Long-term dark incubations of 20-cm thick ice segments, cut from replicate (adjacent in the field) ice cores collected in March, were conducted in freezers at UAF set to temperatures of −5°C, −15°C and −25°C (±2°C) after cores were transported in insulated containers from Barrow to Fairbanks. Three segments, each sealed in a separate zip-lock plastic bag, were incubated at each temperature. Upper colder ice-core segments (from 0 to 20 cm below surface) were held at the colder temperatures (−15°C and −25°C), while lower warmer segments (from depths of 95–115 cm) were held at −5°C. After incubation periods of 0, 114 and 441 d, the ice segments were melted and analyzed for concentrations of EPS and bacteria following protocols outlined above.

2.3. Microscopic analysis of diatoms and brine pockets within the ice

We used a non-invasive method, newly developed by Junge et al. (2001a), for epifluorescent microscopic observations of organisms directly within the pore spaces of sea ice at in situ temperatures. Although this method can be used to analyze a wide range of organisms, particles and ice features, we used it to examine primarily diatoms and their brine pores in bottom ice-core samples (112-cm depth, field temperature of −2°C, collected in March), where diatoms were

numerous enough to enable this type of analysis. After collection and temporary storage at −15°C for 1 week, ice samples were placed at temperatures of −5°C, −15°C and −25°C. Within a period of about 2 weeks, ice sections 5–6 mm thick were prepared and examined under the desired temperature in a temperature-controlled room designed for that purpose (housing the microscope, computer-imaging system, and other required equipment; Junge et al., 2001a). Selected samples from the long-term incubation experiments described above (after the 114-d incubation period) were also prepared and analyzed at −25°C.

These thin ice sections were attached to glass slides with freshwater droplets frozen to the sample perimeter. The surface of each section was removed at 200-μm intervals with a sled microtome, and the process was repeated on the other side of the sample to ensure parallel pristine surfaces before transfer of the sample to the glass slide. For epifluorescent microscopy, ice sections were stained with the DNA-specific stain DAPI. The DAPI-staining solution was prepared and equilibrated for 24 h to the desired temperature and salinity for a final concentration of 20 μg ml^{-1} (see Junge et al., 2001a, for more details). The final, 0.2-μm pre-filtered isothermal–isohaline solution was applied to the microtomed surface of the sample and overlain with a glass coverslip. The sample was allowed to stain for at least 1 h in the dark before microscopic observations commenced.

For both transmitted-light and epifluorescent microscopic analyses, a Zeiss Axioskop 2 microscope was fitted with an epifluorescence illumination system and modified for operation at sub-zero temperatures (to −25°C). The microscope was equipped with optical filter sets for DAPI and autofluorescence (excitation 365, 395 nm beam splitter, longpass emission 420 nm; Lucifer Yellow 425 nm excitation, 540 nm emission, 460 nm beamsplit). Images of diatoms (and a few flagellates) and brine-pore features were captured with a MTI DC330E 3CCD color camera and a Scion CG-7 RGB Color PCI Frame grabber. Pixels were digitized to 8 bits (512 gray levels) for each of the three red–green–blue color channels. Images were stored and analyzed on a G3 Macintosh computer. All images were analyzed with a variant of NIH Image v 1.62a (Rasband and Bright, 1995).

Diatoms were first located inside the ice matrix under transmitted light at 286× magnification (1 pixel 0.3 μm), then analyzed under autofluorescent excitation and DAPI excitation with the appropriate filter set and higher magnification, to 1143× or 3.3 pixels μm^{-1}. Ice-section examination began 10 μm below the ice surface to a total examination depth of about 400 μm, which allowed clear determination of cell structure. Dimensions of diatoms and brine pores were measured at 1143× final magnification; distances between cells and adjacent brine layers, at 286× final magnification.

3. Results

3.1. Field-related measurements

The overall lengths of the March and May ice cores were 115 and 165 cm, respectively (Fig. 1; the November core of newly formed ice for the next winter was 40-cm thick). In situ temperature profiles differed considerably between the March and May cores (Fig. 1a). In March, the ice exhibited a steeper gradient as a result of a lower minimum temperature (−18.6°C in March versus −10.3°C in May) due to colder air temperatures (−40°C). As a consequence of the colder temperatures, brine salinity gradients in March were also steeper, reaching salinities of 200 units in the upper ice (Fig. 1b). Bulk salinity profiles in both cores had typical C-shapes (Fig. 1c), with ranges of 4–6.2 in March and 4–9 in May. Variability in bulk salinity based on three parallel cores averaged 10.1% (range of 2.4–19.1%) per 10-cm ice horizon. Snow cover of the replicate cores ranged from 15 to 20 cm.

Bulk EPS concentrations ranged from 1.00 to 7.71 mg XGEQV l^{-1} in the vertical profiles of the ice cores from March and May (Fig. 1d), with maxima occurring near the ice–water interface in both cases. EPS concentrations in May, however, averaged 4.70 (±1.38) mg XGEQV l^{-1} and were significantly higher (factor of 2.3) than the average in March (2.00±0.94 mg XGEQV l^{-1}). Median

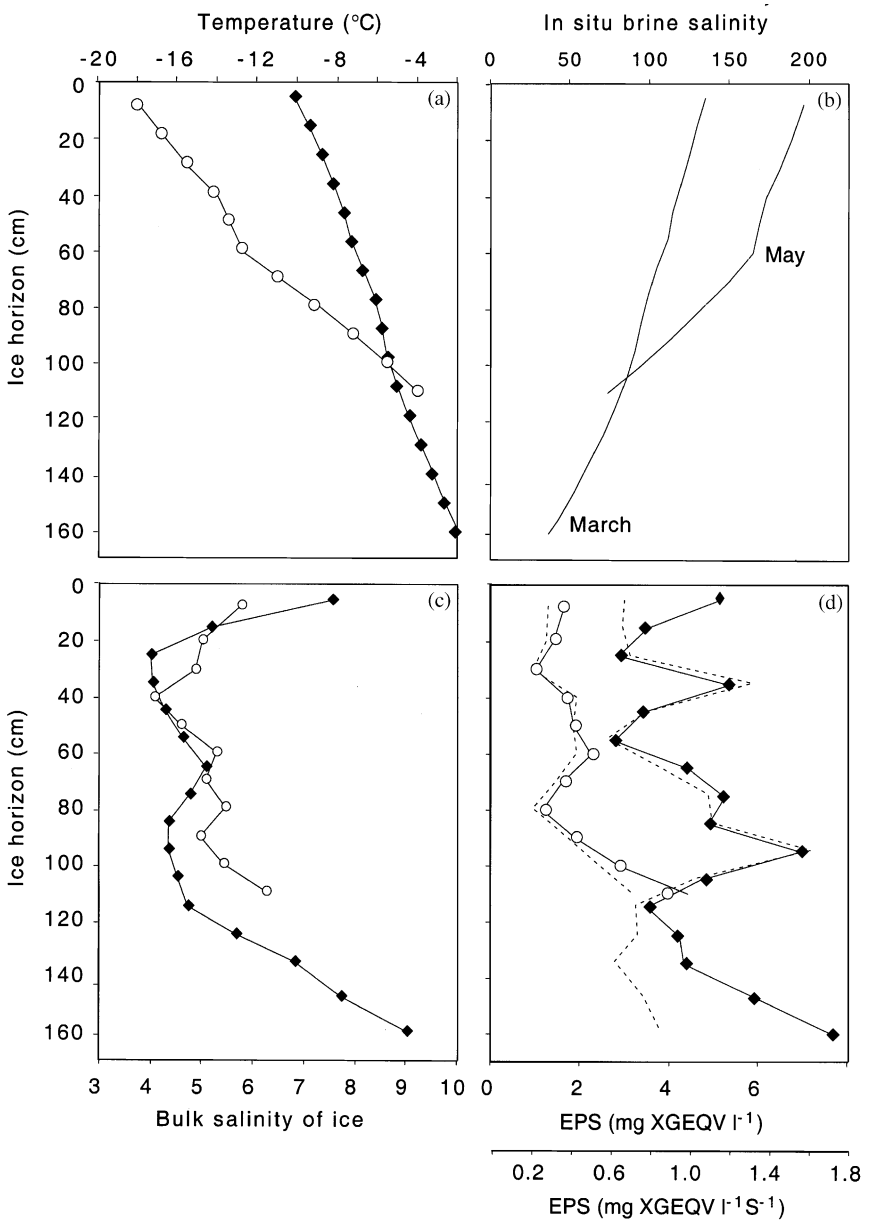

Fig. 1. Vertical profiles of (a) temperature; (b) in situ brine salinity (calculated after Cox and Weeks, 1983; see text); (c) bulk salinity; and (d) EPS concentration (in melted ice segments) scaled to sea-ice volume (solid lines) or to salinity (dotted lines) for cores collected in March (○) and May (◆) of 1999.

values (4.57 and 1.76 mg XGEQV l^{-1}) differed by a similar factor (2.5). Concentrations in newly formed ice in November (excluding a band of anomalous sediment-laden ice caused by storm activity; Stierle et al., 2000) averaged 1.52 ($\pm$0.73) mg XGEQV l^{-1} or about 73% of the average measured in March. Profiles of EPS scaled to bulk salinity (to account for differences in ice structure;

Fig. 1d) did not differ significantly from the bulk EPS profile (mg l^{-1}), except in the uppermost and lowermost sections of the ice cores. DOC concentrations in May ranged from 50.2 to 258 μM (l^{-1} melted ice) at the ice–water interface. The average was 107 (±52.0) μM, and the vertical profile indicated no trend.

Macro-nutrient profiles, based on bulk analyses and scaled to bulk salinity to account for ice structural differences (Fig. 2a; data available for March only), revealed a strong PO_4 maximum near the bottom of the core (depths of 85–115 cm) with a sharp transition to a minimum that plotted higher in the ice at 80 cm (for the ice segment from 75–85 cm), corresponding to an in situ temperature of −9°C; the NO_3 minimum was observed where PO_4 was highest (85–105 cm). The NH_4 profile was relatively featureless and probably biased due to freeze storage of samples (data not shown). The Chl *a* profile (Fig. 2b) revealed highest pigment content (16 μg l^{-1}) in the lowermost ice segment (105–115 cm). Maxima in bacterial abundances occurred in the lowermost ice segment (4×10^7 cells l^{-1}), at 70 cm, and at the ice surface (7×10^7 cells l^{-1}). Profiles of nutrient ratios revealed a zone of marked nitrogen depletion (NO_3/DIN and DIN/PO_4 minima) at 75–105 cm that corresponded with low pigment ratios (Chl *a*/phaeophytin; Fig. 2c). A slight increase in Chl *a* occurred between 70 and 80 cm, which resulted in a high Chl *a* to pheaophytin ratio at 70 cm ice depth. Nitrogen also appeared depleted by virtue of the generally low Redfield ratios for DIN/PO_4 throughout the core, averaging only 24% of the optimum of 15 (Günther et al., 1999). Taken together, the nutrient, bacteria and pigment data indicate a major transition zone for biological activity (ongoing or recent) within the ice that corresponded to in situ temperatures in the range −9°C to −11°C (Fig. 2).

The concentrations of both EPS and DOC scaled to brine volume, and thus reflecting the actual concentrations encountered by the organisms, were observed to increase significantly (Spearman rank correlation one-sided, $p < 0.002$) as a function of colder temperatures in both the March and May cores (Fig. 3). EPS and DOC did not correlate significantly with bulk salinity (or

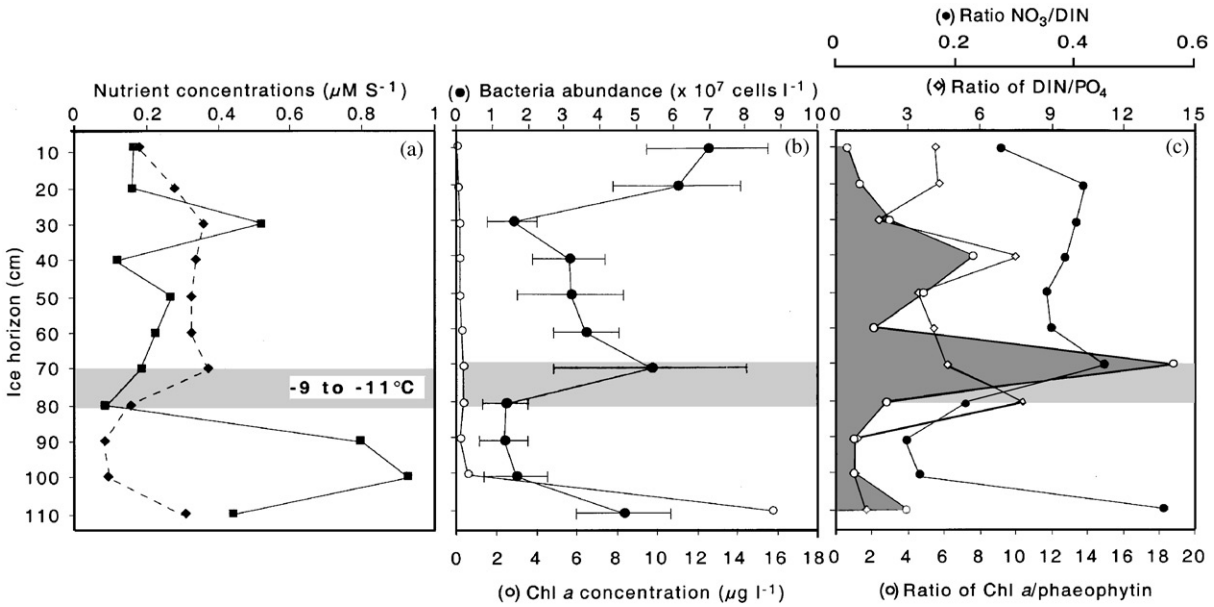

Fig. 2. Vertical profiles of (a) phosphate (■) and nitrate (◆) scaled to ice salinity; (b) bacterial abundance and Chl *a* scaled to sea-ice volume; and (c) ratios of nitrate to total DIN, DIN to dissolved inorganic phosphate, and Chl *a* to phaeophytin in March of 1999. Error bars indicate SD of microscopic counts.

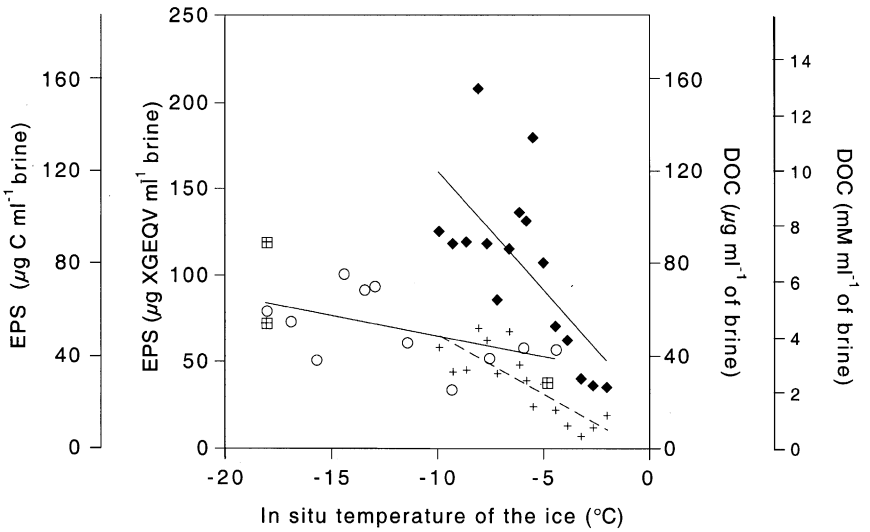

Fig. 3. Relationships between in situ temperature and concentration of EPS (solid lines; (○) March, $r^2 = 0.26$; (♦) May, $r^2 = 0.45$) and DOC (dashed line; ⊞ March, no regression; (+) May, $r^2 = 0.66$) experienced by organisms within the volume of brine of the ice-core segments. EPS values were scaled according to the conversion factor of 0.75 for xanthan gum to carbon (Engel and Passow, 2001). Concentrations are given in both units to allow a comparison of EPS and DOC.

Chl *a*, available for March). In spite of the concentration mechanism inherent to colder in situ temperatures and reduced pore space, as well as the brine dilution by meltwater that occurs naturally as temperatures increase, EPS concentrations in the March brines were always lower than in the May brines for ice segments of equivalent temperature (compare slopes of the two solid lines in Fig. 3). In contrast, DOC concentrations in the brine reached a maximum of 89 µg ml^{-1} (7.4 mM) in the coldest ice (at −18°C in March), yet did not appear to differ from March to May across similar temperature horizons (compare the three values from March with the dotted line for May in Fig. 3). EPS concentrations correlated positively with DOC values in May, when the larger DOC data set was available for comparison (Spearman rank correlation; $n = 16$; $p < 0.01$). Ratios of EPS/DOC, however, decreased at colder temperatures, indicating a relative increase in the DOC fraction (compare slopes for May EPS and DOC data in Fig. 3) rather than the reverse (conversion of DOC to EPS).

In March, bacterial concentrations scaled to brine volume ranged from 0.3×10^6 cells ml^{-1} in a lower portion of the ice (95–105 cm) to 3.3×10^6 cells ml^{-1} in the upper portion (0–15 cm). In May, values ranged from 1.2×10^6 cells ml^{-1}, again in a lower ice segment (140–155 cm), to 8.9×10^6 cells ml^{-1} in an upper segment (10–20c m). Brine concentrations of EPS correlated positively with those of bacterial abundance in both months, and significantly in March (Spearman rank correlation: March, $n = 11$ segments, $p < 0.05$; May, $n = 16$ segments, $p < 0.10$). The mean bacterial abundance in the May ice core, when scaled conventionally to melted ice volume (1.9×10^9 cells l^{-1}), was about half that observed in the March core (3.5×10^9 cells l^{-1}), representing a reduction in the total bacterial population of 46%.

3.2. Long-term incubation of ice-core segments

Time-course measurements of EPS concentrations in ice-core segments (Fig. 4), collected in March and incubated at subzero temperatures in the dark, revealed EPS accumulation rates of 47, 10 and 5 µg XGEQV × l^{-1} d^{-1} at −5°C, −15°C and −25°C, respectively ($n = 3$ in each case;

$r^2 = 0.97$, 0.95 and 0.98, respectively). Triplicate ice sections of the 20–30 cm horizon at the same site and in a nearby lagoon (Elson lagoon, 30–40 cm) revealed coefficients of variation of 0.65 and 0.24, respectively, indicative of moderate variability between cores. The values of EPS during the experimental incubations surpassed this measure of natural spatial variability, given the coefficients of variability for each set of incubated ice samples (0.89, 1.76 and 2.03 at −5°C, −15°C and −25°C, respectively). Use of a traditional multivariable linear regression model (EPS concentration = a1 × time + a2 × temperature) revealed that the coefficient for time is significantly different than zero (p-value for a1 is <0.05), implying that at any temperature the slope will be not zero and hence EPS concentrations increased significantly. Bacterial numbers, however, generally decreased in these samples at all three incubation temperatures (Table 1), with overall losses of 54–76% by the end of the experiment (after 441 d).

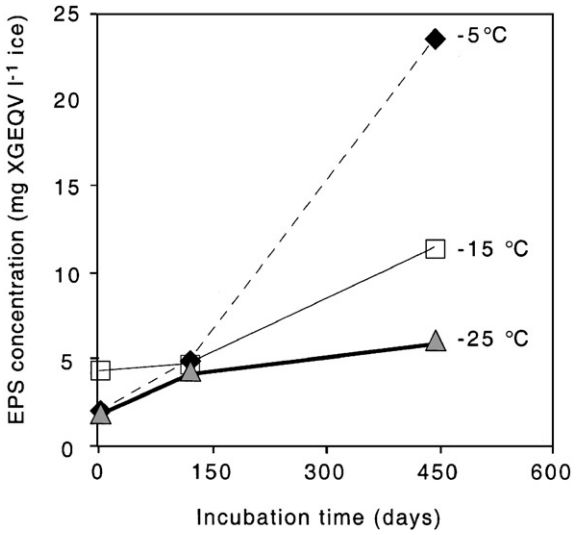

Fig. 4. Increase of EPS in ice segments, from cores collected in March, during long-term incubation in the dark at winter temperatures: (◆) lowermost ice segments (95–115 cm) at −5°C; (□) uppermost ice segments (0–20 cm) at −15°C; and (▲) uppermost ice segments (0–20 cm) at −25°C.

3.3. Microscopic analysis of diatoms and brine pockets within the ice

Qualitative examination of microscopic images of the diatoms (all of which were pennate diatoms) and brine pores within the 112-cm ice horizon (originally at −2°C in the field in March and brought to temperatures of −5°C, −15°C and −25°C within 12 h) revealed several consistent features (Fig. 5a–e). In cases where pore space was minimal or absent, ice crystals had encroached upon the cell and the chloroplast had lost its integrity (Fig. 5b). Where the diatom occupied a pore space larger than itself, the cells appeared physically undamaged and the chloroplasts well preserved (Fig. 5c–e). The walls of some of these brine pores, as well as a pore containing an autotrophic flagellate, showed distinctly jagged or undulating contours (Fig. 5e) interpreted as an effect of an amorphous organic matrix on the shape of the pore. Pores without diatoms (Fig. 5b) had only smooth surfaces. Most of the pores that contained diatoms differed in shape from the cell, such that a direct influence of the cell wall on the pore dimension was not obvious. A staining

Table 1
Number of bacteria ($\times 10^7 l^{-1}$ melted ice ± SD[a]) in ice segments from the long-term incubation experiments (see text)

Incubation time (d)	Incubation temperature (°C)		
	−5	−15	−25
0	9.1 (±2.9)	8.7 (±1.2)	7.5 (±1.8)
118	5.7 (±1.9)	9.7 (±3.3)	1.9 (±0.6)
441	4.1 (±1.9)	2.1 (±1.5)	2.2 (±1.7)
Reduction to	44%	24%	33%

[a] Based on replicate counts of fields on a filter, where $n = 20$ fields.

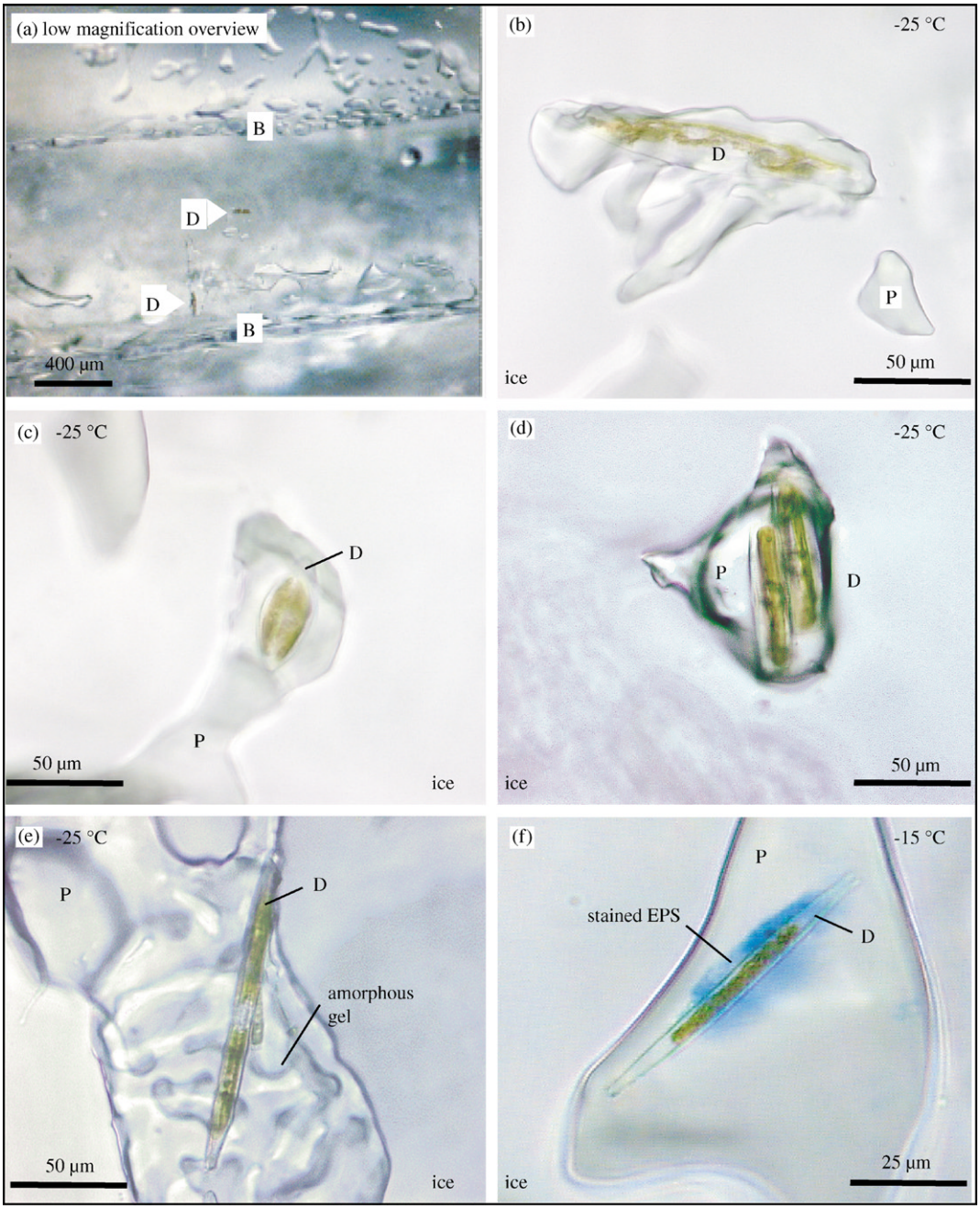

Fig. 5. Microphotographs of pennate diatoms residing within pore spaces at a depth of 112 cm in an ice core collected in March of 1999 after cooling from in situ temperature to −25°C: (a) low-magnification image showing ice texture, brine layers (B) and diatoms (D); (b) damaged diatom cell in a pore with encroaching ice crystals and an empty pore space (P); (c) diatom in a pore connected to a brine layer; d) two diatoms in an isolated pore; (e) diatom in a pore with indications of amorphous transparent gel-like exopolymeric material; and (f) diatom surrounded by an EPS matrix successfully stained with Alcian blue (at −2°C prior to chilling to −15°C).

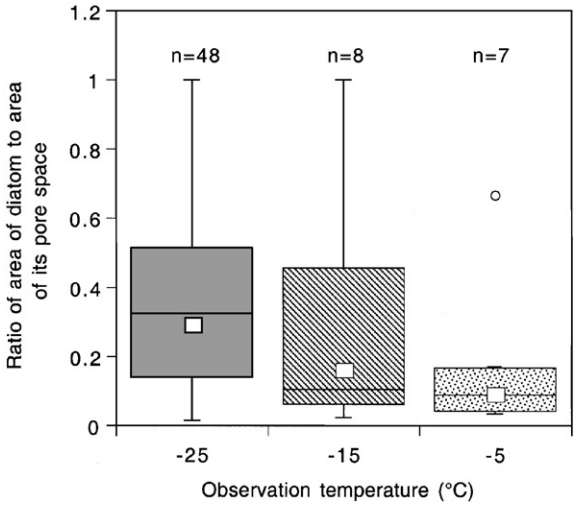

Fig. 6. Relation of cross-sectional areas of diatoms to pores at different temperatures. The mean ratios, 5, 25, 75 and 95 percentiles, and data (○) falling outside these percentiles are given, along with expected reduction in pore space around the cells (□) according to the volume fraction reduction of brine (Cox and Weeks, 1983).

success of EPS-enveloped diatoms at the same sampling site and relative location in the ice in June 2001 is illustrated in Fig. 5f.

Most of the diatoms were located within pores large enough to easily accommodate the cells, despite the temperature-dependent reduction in volume of sea-ice brines (Fig. 6). The ratio of the cross-sectional area of the diatom cell to that of its pore space increased at colder temperature (at −5°C, −15°C and −25°C; Fig. 6), following the expected inverse relation of the reduction in brine volume at decreasing temperature (Cox and Weeks, 1983). Even at −25°C diatoms remained surrounded by sufficient brine fluid to accommodate the size of the cell (pore area 3 × the area of the diatom). The smallest diatoms, less than 183 μm in length, always occurred in pores significantly exceeding their size.

In summarizing these microscopic observations (Table 2), we calculated that 47% of the diatoms examined contained intact autofluorescent chloroplasts. Of the remaining cell chloroplasts observed, 17% were plasmolyzed. Although the new DAPI-staining method we used underestimates the total number of DNA-containing cells within an ice section (because the dye penetrates only into pores connected to the microtomed surface of the thin section being examined; Junge et al., 2001a), 29% of the diatoms observed were stained with DAPI. Only 6% of the diatom cells (whether stained or not) were damaged or crushed, while only 2% were situated in pores of the same dimensions as their body size (no obvious brine pocket). Of the pores examined, 8% had jagged or undulating contours.

The position of diatoms in their individual pore spaces relative to the center of nearby brine layers averaged a distance of 276 μm (SD = ±150 μm, $n = 191$; Fig. 7); the brine layers themselves were spaced at a median distance of 789 μm (range of 477–1383 μm, $n = 21$; Fig. 7). Frequently, a connection between the pore and the adjacent brine layer could be visualized (Fig. 7). Diatoms were never found within a brine layer, indicating that the organisms did not migrate with the advancing crystal interface during the imposed freezing

Table 2
Microscopic observations of healthy and damaged diatoms[a] and features of their microhabitats within ice-core sections collected in March of 1999 (see text for details)

Observed feature	Number of observed features/total diatoms observed	Percentage of total diatoms observed
For healthy diatoms		
Autofluorescent chloroplasts	60/129	46.5
DAPI stained	50[b]/171	29.2[b]
For damaged diatoms		
Plasmolyzed chloroplasts	31/178	17.4
Crushed cells	11/178	6.2
Of the microhabitat		
Signs of altered brine pocket	15/178	8.4
No obvious brine pocket	4/178	2.2

[a] Only diatoms visible in clear focal plane under the microscope were analyzed.
[b] Underestimate, since DAPI stain penetrates only into open pores on the microtomed surface of the ice section.

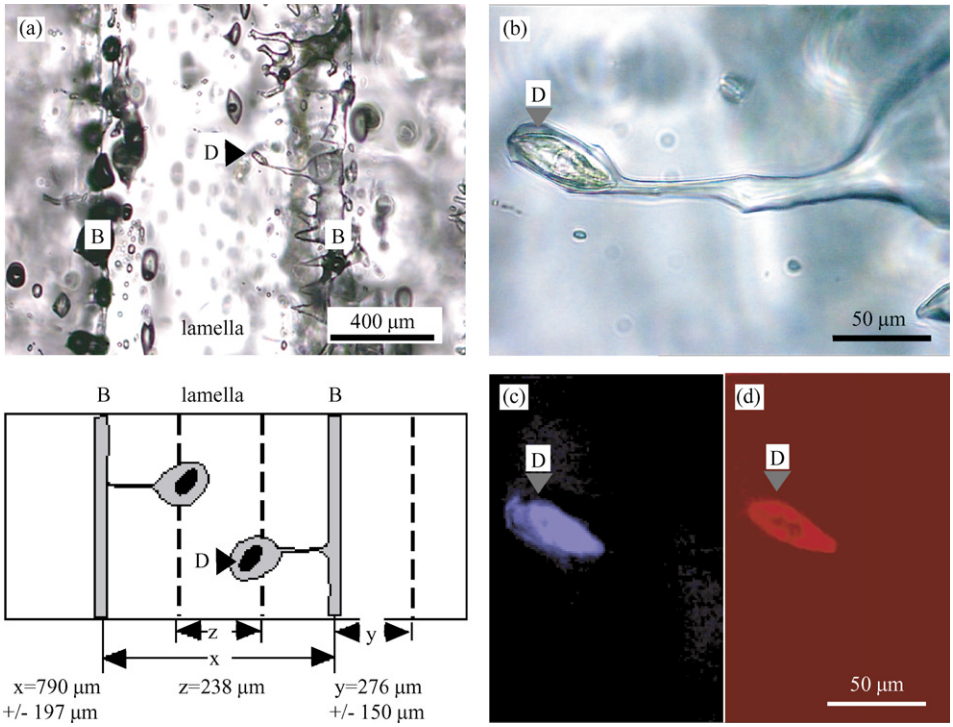

Fig. 7. Microphotograph of pennate diatom (D) inside a brine pore connected to a brine layer (B) in the skeletal layer in March 1999 at 112-cm depth: (a) low-magnification microscopic images using transmitted light; (b) identical photo at high magnification; (c) with blue light excitation showing DAPI-stained nucleus; and (d) with Chl *a* excitation showing chloroplast. Included is a schematic representation of (x) average measured distance of lamella thickness at −25°C; (y) average measured distance of diatoms to the edge of the lamellae (dashed lines); and (z) calculated average distance of frozen-in diatoms from one to the other side of the crystal lamellae at −2°C ($z = x - 2y$).

process. The orientation of pennate diatoms in the horizontal plane of an ice section was anisotropic, with a median intersecting angle of 29° (range of 0.5–90°, $n = 252$) between cell length and brine layer axes, presumably a reflection of the relatively rapid (within 12 h) freezing process.

4. Discussion

Prior to this study, Krembs and Engel (2001) had demonstrated that summer pack ice in the Arctic carries large quantities of EPS near the ice–water interface, organic materials that might in turn contribute significantly to aggregate formation in the water column (e.g., Passow et al., 1995). The vertical EPS profiles that we obtained for other times of the year (November, March and May) in this study now demonstrate that EPS occurs in all horizons of the ice and in concentrations comparable in magnitude (in terms of XGEQV) to the highest reported elsewhere in the marine environment; i.e., in Antarctic waters during *Phaeocystis* blooms (Hong et al., 1997) and in the Adriatic Sea (e.g., Engel, 1998). The significance to the ocean carbon budget of "transparent particles," a form of EPS consisting largely of polysaccharide molecules in the particulate phase larger than 0.4 µm, has been well recognized for temperate oceans (Alldredge et al., 1993; Grimm et al., 1997). To place our sea-ice results into a broader carbon context, we converted EPS from weight units of XGEQV (Fig. 1d) to carbon units (e.g., Fig. 3) via the empirical equation by Engel and Passow (2001). Implicit to use of their equation is the assumption that

diatoms were the source of EPS in our ice samples. The observed correlation between diatoms and EPS in Laptev Sea ice by Krembs and Engel (2001), as well as arguments made below, supported this assumption. Given the measured ice thicknesses near Barrow, we estimated the areal EPS-carbon content of the ice to be 1.5–1.9 g C m^{-2} in March and 3.3–4.0 g C m^{-2} in May (the full range being 0.6 to 5.4 g C m^{-2}). These estimates are similar to average DOC concentrations in the ice in March and May (1.3 g DOC m^{-2}) and to DOC concentrations in winter sea ice of the Eurasian sector of the Arctic in 1993 (Thomas et al., 1995). They are equivalent in magnitude to the average particulate organic carbon (POC) content of the ice measured in March at our study site (1.5 g C m^{-2}, range of 1.2 to 2.3 g C m^{-2}; Eicken et al., 1999). Considered in light of the recent estimate of 8.6 g C m^{-2} year for Arctic summer ice-algae production (Gosselin et al., 1997), these carbon stock estimates are notably high, presumably because of the proximity of the sampling site to shore. Despite the operational overlap of 0.3 μm in pore sizes between EPS (>0.4 μm) and DOC (<0.7 μm) measurements, EPS-carbon appears to be a significant pool of organic carbon in the Chukchi Sea winter sea ice near Barrow, potentially exceeding other pools of carbon in the ice. Though our data set is geographically and spatially limited and may reflect local variability in productivity over the shelf regions of the Chukchi Sea (e.g., Alexander et al., 1973; Hillman, 1984; Hansell et al., 1993), EPS may be similarly important in other Arctic shelf regions, where EPS released from melting sea ice in aggregated form (Krembs and Engel, 2001) could figure significantly in carbon export to deeper regions of the Arctic Ocean.

With regards to the source of EPS in winter sea ice, the presence of significant quantities in November suggests either that seawater-EPS was incorporated into the ice during fall ice formation or that EPS was produced within the ice shortly after its formation. Although we do not have concurrent measures of seawater-EPS from our study site, earlier work there has shown that primary productivity and Chl *a* concentrations in the water column are typically low (Alexander et al., 1973), while EPS concentrations in seawater below the summer pack ice in the Laptev Sea were lower than in sea ice typically by a factor of ten (Krembs and Engel, 2001). These observations argue against seawater as the sole or primary source of EPS to the ice. In contrast, we do have evidence for significant aphotic production of EPS within the ice at representative wintertime temperatures, to -25°C, from our sea-ice incubation studies (Fig. 4). We cannot yet explain with certainty the mechanism of EPS production, but an abiotic transformation of dissolved mucopolysaccharides to gels via freeze–concentration of the brine is not supported by the observed decrease in ratios of EPS/DOC with decreasing temperature (Fig. 4). Nor was EPS production in the incubation experiments confined to the initial freezing process (as samples were brought to test temperatures), as might be predicted for a physical–chemical process. The physical–chemical behavior of organic molecules in a brine environment characteristic of winter sea ice, however, remains poorly understood and may have influenced the kinetics of EPS-gel formation in ways not recognizable in our experiments. Evidence for a biological source of the EPS accumulation observed in the nearly impermeable ice of our experiments (< -5°C; Freitag, 1999) comes from a consideration of the similarity in DOC concentrations between March and May, but overall higher EPS concentrations in May (Fig. 3). Assuming that the total carbon pool in the interior of the ice between March and May was unchanged because of impermeability of the ice, then the EPS must have originated from the POC pool instead, which includes internal pools of organisms. However, cell lysis due to cryo-damage, thus releasing intracellular EPS content, is not consistent with the temperature-based patterns in the EPS/DOC ratios we measured in March and May (Fig. 3), the gradual nature of the increase in EPS over the extended period of our incubation experiments (Fig. 4), or the healthy state of the majority of diatoms observed microscopically (Table 2, Figs. 5 and 7). We suggest instead that sea-ice organisms produced or released EPS during the long-term winter simulations and during the field season (between our March and May cores), in the latter

case as physiological activity increased in a gradually warming ice. The responsible organisms must have been bacteria or diatoms, either utilizing internal energy reserves such as glycolipids produced under stress (e.g., Mock and Gradinger, 2000) or engaged in production, since other organisms were rarely seen in our ice samples.

Given the correlation between bacterial abundance and EPS in the March core and recent reports of their continuing metabolic activities in various types of ice at temperatures as low as −20°C (Carpenter et al., 2000; Junge et al., 2001b), we first considered bacteria as the primary agents of EPS production in our cores. No other lines of evidence, however, seemed to support this possibility. The correlation between bacterial and EPS concentrations did not hold up in the May core, and bacterial populations decreased during the long-term incubation experiments (Table 1). To examine whether an active conversion of bacterial carbon to EPS may have occurred, perhaps due to high stress levels, we considered the published rates for bacterial EPS production (available only for warmer waters) of 7.1 ($\pm$3.3) amol C cell^{-1} l^{-1} h^{-1} (Stoderegger and Herndl, 1998). The maximal production rate we could then calculate for the bacterial population sizes in our sea-ice samples was 0.19 μg C l^{-1} d^{-1}, falling well short of even the slowest rate observed in the long-term incubation experiments (3.8 μg C l^{-1} d^{-1}).

Turning to diatoms, we used the range of published rates for their EPS production (Underwood and Smith, 1998), albeit at warmer temperatures (again, no cold-temperature rates are available), and the Chl *a* concentration of 16 μg l^{-1} measured in March (representative for this time of year and location; Alexander et al., 1973) to calculate an EPS production range of 19–61 μg C l^{-1} sea ice d^{-1}. These rates greatly exceed the maximum calculable rate for bacterial EPS production (even the most conservative rates based on lowest Chl *a* values were considerably higher than the maximal bacterial rate). They also overlap with the range observed in our long-term incubation experiments (3.8–35 g C l^{-1} d^{-1}) and with the production rate calculable from the field data (Fig. 1d) between March and May (36.6 μg C l^{-1} d^{-1}). Note that we found good agreement (88%) between experimental EPS production rates and in situ EPS increases between March and May, assuming a gradual temperature increase in the ice. Diatoms thus emerge as the best candidate organisms to explain the EPS produced in our ice samples. One scenario is that during freezing, and while encased by ice crystals, diatoms experience reduced nutrient availability (Gleitz et al., 1995) and respond with elevated EPS production as occurs at the end of a planktonic diatom bloom. Eventually, they reach the physiological limits of activity, currently reported for diatoms and flagellates at −8°C (e.g., Kottmeier and Sullivan, 1990; Aletsee and Jahnke, 1992; Stoecker et al., 1997).

Evidence of biological activity in sea-ice samples is generally reflected in downcore profiles of inorganic nutrient concentrations and ratios. Wintertime profiles, however, are rare (Gleitz et al., 1995) and not easily interpreted at the scale of the organism. The nutrient and Chl *a* concentrations and ratios that we measured in March (Fig. 2) generally fall within the range of values reported earlier for this time and location (Alexander et al., 1973). The high PO_4 concentrations (and thus low DIN/PO4 ratios), indicative of nutrient regeneration in sea ice (Gradinger et al., 1992; Mock and Gradinger, 2000), that we observed in the lower segments of the ice (below 80 cm) are consistent with the understanding that nutrient regeneration requires a certain degree of interconnectivity of pore space for an organism to access its prey (Krembs et al., 2000a, b). The pronounced peak in the Chl *a*/phaeophytin ratio above the 80-cm horizon (Fig. 2c) may be attributable to physiologically active diatoms, sequestered in individual brine pores as a result of the effect of our winter observation temperatures on ice structure (Fig. 7). The detection of primary production in March in the middle of the ice from our study area, reported by Alexander et al. (1973), supports this suggestion, as does the elevation in bacterial numbers near this horizon (Fig. 2b). The alternative possibility, that this horizon reflects the remnants of a former algal bloom incorporated from the water column or a former ice–water interface, is not tenable, since the

last contact of this horizon with the water occurred during the darkest months of the year and an allochthonous source of organic detritus would register a higher pheaophytin content than observed in our profiles. Furthermore, a transition in the nutrient ratios of NO_3/DIN and DIN/PO_4 also occurred near the 80-cm ice horizon, where the corresponding temperature was −9°C to −11°C (Fig. 2c), consistent with the lower physiological bounds of sea-ice diatoms and flagellates (−8°C; Aletsee and Jahnke, 1992; Stoecker et al., 1997). If temperature limitation is critical for biological EPS production, then the observed warming of the ice sheet between March and May above −10°C (Fig. 1a) and the higher EPS concentrations (Fig. 1d) may be linked to an awakening in physiological activity during late winter.

Attempts to stain EPS in the pores of ice sections at winter temperatures with Alcian blue or Ruthenium red failed because of the inhibiting effects of high brine salinities on the binding efficiency of the stains. However, in situ staining of the ice at −2°C prior to chilling directly confirms the link between diatoms and EPS production (Fig. 5f). The shape of the ice pores under winter temperatures (Figs. 5 and 7), their consistently large size relative to the encased diatoms (Fig. 6), and literature reports on diatom–mucus associations (Sullivan and Palmisano, 1984; Smith et al., 1998; Smith and Underwood, 2000) also indirectly support this link. Initial studies using artificial sea ice have revealed that EPS enrichment caused salt retention within the ice (Krembs et al., 2000a, b), which increases the liquid brine fraction and, hence, the habitable pore space at any given temperature. If organisms maintain high local concentrations of EPS at the cell periphery, then salt retention could explain the observed high number of diatoms in this study that were sequestered in sufficiently large pores, though they followed the overall thermodynamical volume reduction during cooling (Fig. 6). Microscopic observations directly within sea-ice sections revealed that a majority of the diatom cells in these pores were of high morphological integrity at temperatures to −25°C, further linking EPS to cell health at winter temperatures and salinities.

Ackley et al. (1987) proposed that diatoms must have a means of adhesion to ice crystals. If EPS around diatoms allow the cells to adhere to the advancing ice crystals under winter conditions, then EPS will also change the diffusive properties of salt at the interface, creating local defects in the advancing ice crystal. Such defects could be expected to evolve into mucus-filled pockets as the crystals widened laterally. Continued freeze-concentration would remove water from the EPS-gel that anchors, immobilizes and cushions the cell within the gradually forming brine pore. While the positive role of sugars in enhancing the viability of frozen specimens is well known (e.g., Taylor and Fletcher, 1998) and the ice-pitting effects of extracellular diatom proteins have been described (Raymond et al., 1994), our observations support a new extracellular mechanism of cell protection linked to polysaccharides (EPS). Diatoms subjected to short-term (12 h) cooling in sea ice from −2°C to −25°C were located inside individual brine pores at an average distance of about 280 μm from a brine layer (Fig. 7). In about a third of these cases, the pores were still connected to the brine layer. For diatoms to have actively colonized these individual pores of limited access at a later stage is unlikely. The close overlap of our observations at −15°C and −25°C (Figs. 5a, and 7a) with the theoretical position of diatoms frozen into a progressively increasing ice-lamella of the skeletal layer (average thickness of 200 μm at −2°C; Jetzek et al., 1990) strongly supports the pore-formation mechanism during crystal growth. Given initial diatom attachment to the crystal surfaces at −2°C, their positions from a brine layer after chilling to −25°C, and the average distance between layers at that temperature (Fig. 7), the diatoms that we observed must have remained adhered to the crystal lamella for a duration of at least 4 months.

We suggest that EPS is an important extracellular substance aiding in winter survival of sea-ice organisms and should be considered in addition to intracellular adaptations to cold temperatures and high salinities (e.g., Hargens and Shabica, 1973; Murase, 1992; Knight and DeVries, 1994; Kirst and Wiencke, 1995; Kawahara et al., 1996). A large pool of polyhydroxyl compounds, capable

of depressing the homogeneous nucleation temperature of water with non-colligative effects (Franks et al., 1977; Sutton, 1991; Murase, 1992), is clearly present in winter sea ice. Their presence could figure significantly in altering the sea-ice habitat on the ambit of the organisms and on larger scales (Krembs et al., 2000a, b). Food polymers display an amorphous, non-equilibrium state during ice formation (Roos, 1995) when water content critically controls the crystallization of the matrix. For example, a xanthan gum content of 50% by weight reduces the freezing temperature of freshwater to about –13°C (Yoshida et al., 1990, 1992; Murase, 1992). Our reported EPS concentrations (Fig. 1d), which conservatively assume a homogeneous distribution in the brine, could be orders of magnitude higher around the cells with similar effects as food polymers. In the context of known bacterial strategies (Kawahara et al., 1996), effects of algal exudates on sea ice and its brine environment could further our understanding of extracellular mechanisms deployed by microorganisms in the presence of ice nucleators.

In conclusion, concentrations of EPS in sea ice are high enough to play an important role in the marine Arctic carbon budget following ice melt. Converging lines of evidence point to wintertime EPS production within the ice by diatoms. On the microscale, within relatively spacious pores even under severe temperatures, they appear to provide effective protection to diatoms against the harsh environmental conditions of the season and may be responsible for the creation and maintenance of adequate habitable pore spaces and the positioning of cells within them.

Acknowledgements

This work was supported by NSF-LExEn awards OPP-9817738 and OPP-9809468 to Deming and Eicken and OPP-0085457 to Deming, Eicken and Krembs, with additional support from the University of Washington Astrobiology Program. Our work in Barrow benefited greatly from logistical support by the Barrow Arctic Science Consortium (BASC) and, in particular, from help provided by D. Ramey. We also thank L. Shapiro and S. Carpenter for help with the field program. The editor wishes to acknowledge the assistance of Evelyn and Barry Sherr in the processing of the manuscript.

References

Ackley, S.F., Dieckmann, G., Shen, H., 1987. Algal and foram incorporation into new sea ice. EOS 68, 1736.

Aletsee, L., Jahnke, J., 1992. Growth and productivity of the psychrophilic marine diatoms *Thalassiosira antarctica* Comber and *Nitzschia frigida* Grunow in batch cultures at temperatures below the freezing point of sea water. Polar Biology 11, 643–647.

Alexander, V., Horner, R., Clasby, C., 1973. Metabolism of Arctic sea ice organisms. Institute of Marine Science, University of Alaska, Fairbanks, Alaska. IMS report R74-4, p. 120.

Alldredge, A.L., Crocker, K.M., 1995. Why do sinking mucilage aggregates accumulate in the water column? The Science of the Total Environment 165, 15–22.

Alldredge, A.L., Passow, U., Logan, B.E., 1993. The abundance and significance of a class of large, transparent organic particles in the ocean. Deep-Sea Research I 40, 1131–1140.

Bronstein, V.L., Itkin, Y.A., Ishkov, G.S., 1981. Rejection and capture of cells by ice crystals on freezing aqueous solutions. Journal of Crystal Growth 52, 345–349.

Carpenter, E.J., Senjie, L., Capone, D.G., 2000. Bacterial activity in South Pole snow. Applied Environmental Microbiology 66, 4514–4517.

Chin, W.C., Orellana, M.V., Verdugo, P., 1998. Spontaneous assembly of marine dissolved organic matter into polymer gels. Nature 391, 568–572.

Cooksey, K.E., Wigglesworth-Cooksey, B., 1995. Adhesion of bacteria and diatom to surfaces in the sea: a review. Aquatic Microbial Ecology 9, 87–96.

Costerton, J.W., Lewandowski, Z., Caldwell, D.E., Korber, D.R., Lappin-Scott, H.M., 1995. Microbial biofilms. Annual Reviews of Microbiology 49, 711–745.

Cox, G.F.N., Weeks, W.F., 1983. Equations for determining the gas and brine volumes in sea-ice samples. Journal of Glaciology 29, 306–316.

Decho, A.W., 1990. Microbial exopolymer secretions in ocean environments: their role(s) in food webs and marine processes. Oceanographic Marine Biological Annual Reviews 28, 73–153.

Decho, A.W., 2000. Microbial biofilms in intertidal systems. Continental Shelf Research 20, 1257–1273.

Deming, J., Baross, J., 2001. Search and discovery of microbial enzymes from thermally extreme environments in the ocean. In: Dick, R.P., Burns, R.G. (Eds.), Enzymes in the Environment. Marcel Dekker, New York, pp. 327–362.

Eicken, H., Deming, J., Krembs, C., Stierle, A., Junge, K., Bock, C., Miller, H., 1999. Morphology and microphysics of sea-ice brine inclusions and their importance for fluid transport and microbial activity. Abstract, American Geophysical Union Annual Meeting, December 1999, San Francisco, USA.

Eicken, H., Bock, C., Wittig, R., Miller, H., Poertner, H.-O., 2000. Nuclear magnetic resonance imaging of sea ice pore fluids: methods and thermal evolution of pore microstructure. Cold Regions Science and Technology 31, 207–225.

Engel, A., 1998. Bildung, Zusammensetzung und Sinkgeschwindigkeit mariner Aggregate. Ph.D. Thesis, Berichte aus dem Institut für Meereskunde an der Christian-Albrechts-Universität, Kiel, p. 145.

Engel, A., Passow, U., 2001. The carbon and nitrogen content of transparent exopolymer particles (TEP) derived from exudates of marine diatoms. Marine Ecology Progress Series 219, 1–10.

Evans, C.A., O'Reilly, J.E., Thomas, J.P., 1987. A handbook for the measurement of chlorophyll *a* and primary production. SCAR Biomass Research Series Handbook 8, 1–114.

Franks, F., Asquith, M.H., Hammond, C.C., Skaer, H.B., Echlin, P., 1977. Polymeric cryoprotectants in the preservation of biological ultrastructure. I. Low temperature states of aqueous solutions of hydrophilic polymers. Journal of Microscopy 110, 223–238.

Freitag, J., 1999. The hydraulic properties of Arctic sea-ice implications for the small scale particle transport. Berichte zur Polarforschung, 325, 150pp.

Giannelli, V., Thomas, D.N., Kennedy, H.A., Dieckmann, G.S., Kattner, G., Haas, C., 2001. The behavior of dissolved organic matter during sea ice formation. Annals of Glaciology 33, 317–321.

Gleitz, M., Vonderloeff, M.R., Thomas, D.N., Dieckmann, G.S., Millero, F.J., 1995. Comparison of summer and winter in organic carbon, oxygen and nutrient concentrations in Antarctic sea ice brine. Marine Chemistry 51, 81–91.

Golden, K.M., Ackley, S.F., Lytle, V.I., 1998. The percolation phase transition in sea ice. Science 282, 2238–2241.

Gosselin, M., Levasseur, M., Wheeler, P.A., Horner, R.A., Booth, B.C., 1997. New measurements of phytoplankton and ice algal production in the Arctic ocean. Deep-Sea Research II 44, 1623–1644.

Gradinger, R., Spindler, M., Weissenberger, J., 1992. On the structure and development of Arctic pack ice communities in Fram Strait: a multivariate approach. Polar Biology 12, 727–733.

Grimm, K.A., Lange, C.B., Gill, A.S., 1997. Self-sedimentation of phytoplankton blooms in the geologic record. Sedimentary Geology 110 (3–4), 151–161.

Günther, S., Gleitz, M., Dieckmann, G.S., 1999. Biogeochemistry of Antarctic Sea ice: a case study on platelet layers at Drescher Inlet, Weddell Sea. Marine Ecological Progress Series 177, 1–13.

Hansell, D.A., Whitledge, T.E., Goering, J.J., 1993. Patterns of nitrate utilization and new production over the Bering–Chukchi shelf. Continental-Shelf-Research 13 (5–6), 601–627.

Hargens, A.R., Shabica, S.V., 1973. Protection against lethal freezing temperatures by mucus in an Antarctic limpet. Cryobiology 10, 331–337.

Heissenberger, A., Herndl, G.J., 1994. Formation of high molecular weight material by free living marine bacteria. Marine Ecological Progress Series 57, 207–217.

Helmke, E., Weyland, H., 1995. Bacteria in sea ice and underlying water of the eastern Weddell Sea in midwinter. Marine Ecological Progress Series 117, 269–287.

Hillman, S.R., 1984. Near-shore chlorophyll concentrations in the Chukchi Sea. Polar Record 22 (137), 182–186.

Hoagland, K.D., Rosowski, J.R., Gretz, M.R., Roemer, S.R., 1993. Diatom extracellular polymeric substances: function, fine structure, chemistry, and physiology. Journal of Phycology 29, 537–566.

Hong, Y., Smith, W.O., White, A.M., 1997. Studies on transparent exopolymer particles (TEP) produced in the Ross Sea (Antartica) and by *Phaeocystis antarctica* (Prymnesiophyceae). Journal of Phycology 33, 368–379.

Horner, R.A., 1996. Ice algal investigations: historical perspective. Proceedings of the NIPR Symposium. Polar Biology 9, 1–12.

Horner, R.A., Ackley, S.F., Dieckmann, G.S., Gulliksen, B., Hoshiai, T., Legendre, L., Melnikov, I.A., Reeburgh, W.S., Spindler, M., Sullivan, C.W., 1992. Ecology of sea ice biota. 1. Habitat, terminology, and methodology. Polar Biology 12, 417–427.

Hung, W.T., Chang, I.L., Hong, S.G., Young, J.D., Chen, G.W., Lee, D.L., 1996. Floc migration and chemical composition change in a freezing chamber. Journal of Environmental Science and Health Part A: Environmental Science and Engineering and Toxic and Hazardous Substance Control 31, 1053–1066.

Jetzek, K.C., Stanton, T.K., Gow, A.J., Lange, M.J., 1990. Acoustical and morphological properties of undeformed sea ice, laboratory and field results. In: Ackley, S.F., Weeks, W.F. (Eds.), Sea Ice Properties and Processes. Proceedings of the W.F. Weeks Sea Ice Symposium, San Francisco, December 1988. US Army Cold Regions Research and Engineering Laboratory, Monograph, pp. 67–75.

Junge, K., Krembs, C., Deming, J., Stierle, A., Eicken, H., 2001a. A microscopic approach to investigate bacteria under in-situ conditions in sea-ice samples. Annals of Glaciology 33, 304–310.

Junge, K., Eicken, H., Deming, J.W., 2001b. An Arctic wintertime study of sea-ice bacteria: abundance, activity and diversity at in-situ temperatures of -2 to -20°C. Abstract, ASM Annual Meeting, Orlando, Florida, May.

Kawahara, H., Ikugawa, H., Obata, H., 1996. Isolation and characterization of a marine ice-nucleating bacterium, *Pseudomonas* sp. KUIN-5, which produces cellulose and secretes it into the culture broth. Bioscience, Biotechnology Biochemistry 60 (9), 1474–1478.

Kirst, G.O., Wiencke, C., 1995. Ecophysiology of polar algae. Journal of Phycology 31, 181–199.

Knight, C.A., DeVries, A.L., 1994. Effects of a polymeric, nonequilibrium "antifreese" upon ice growth from water. Journal of Crystal Growth 143, 301–310.

Kottmeier, S.T., Sullivan, C.W., 1990. Bacterial biomass and production in pack ice of Antarctic marginal ice edge zones. Deep Sea Research I 37 (8A), 1311–1330.

Krembs, C., Engel, A., 2001a. Abundance and variability of microorganisms and TEP across the ice–water interface of melting first-year sea-ice in the Laptev Sea (Arctic). Marine Biology 138, 173–185.

Krembs, C., Gradinger, R., Spindler, M., 2000b. Implications of brine channel geometry and surface area for the interaction of sympagic organisms in Arctic Sea ice. Journal of Experimental Marine Biology and Ecology 243, 55–80.

Krembs, C., Junge, K., Deming, J.W., Eicken, H., 2000b. First observations on concentration and potential production and fate of organic polymers in winter sea ice from the Chukchi Sea. Abstract, International Symposium on Sea Ice and its Interactions with the Ocean Atmosphere and Biosphere, Fairbanks, Alaska, USA, 19–23 June 2000.

Marion, G.M., Grant, S.A., 1994. FREZCHEM: a chemical-thermodynamic model for aqueous solutions at subzero temperatures. CRREL Special Report 94–18, 35pp.

Maykut, G.A., 1985. The ice environment. In: Horner, R.A. (Ed.), Sea Ice Biota. CRC Press, Boca Raton, FL, pp. 21–82.

McConville, M.J., 1985. Chemical composition and biochemistry of sea ice microalgae. In: Horner, R.A. (Ed.), Sea Ice Biota. CRC Press, Boca Raton, FL, pp. 105–129.

McConville, M.J., Wetherbee, R., Bacic, A., 1999. Subcellular location and composition of the wall and secreted extracellular sulphated polysaccharides/proteoglycans of diatom *Stauroneis amphioxys* Gregory. Protoplasma 206, 188–200.

Mock, T., Gradinger, R., 2000. Changes in the photosynthetic carbon allocation in algal assemblages of Arctic sea ice with decreasing nutrient concentrations and irradiance. Marine Ecological Progress Series 202, 1–11.

Murase, N., 1992. Ice crystallization in biological systems. In: Maeno, N., Hondoh, T. (Eds.), Physics and Chemistry of ice. Hokkaido University Press, Sapporo, pp. 245–248.

Okutani, K., 1985. Isolation and fractionation of an extracellular polysaccharide from marine vibrio. Bulletin of the Japanese Society of Fish Nissuishi 51 (3), 493–496.

Palmisano, A.C., Sullivan, C.W., 1985. Growth, metabolism and dark survival in sea ice microalgae. In: Horner, R.A. (Ed.), Sea Ice Biota. CRC Press, Boca Raton, FL, pp. 131–146.

Passow, U., Alldredge, A.L., 1995. A dye-binding assay for the spectrophotometric measurement of transparent exopolymer particles (TEP). Limnology and Oceanography 40 (7), 1326–1335.

Passow, U., Kozlowski, W., Vernet, M., 1995. Palmer LTER: temporal variability of transparent exopolymer particles in Arthur Harbor during the 1994–1995 growth season. Antarctic Journal of the United States 30 (5), 265–266.

Porter, K.G., Feig, Y.S., 1980. The use of DAPI for identifying and counting aquatic microflora. Limnology and Oceanography 25, 943–948.

Rasband, W.S., Bright, D.S., 1995. NIH Image: a public domain image processing program for the macintosh. Journal of Microbeam Analysis 4, 137–149.

Raymond, J.A., Sullivan, C.W., DeVries, A.L., 1994. Release of an ice-active substance by Antarctic sea ice diatoms. Polar Biology 14 (1), 71–75.

Riebesell, U., Schloss, I., Smetacek, V., 1991. Aggregation of ice algae during sea ice melting in the NW Weddell Sea. Polar Biology 1, 239–248.

Roos, Y., 1995. Characterization of food polymers using state diagrams. Journal of Food Engineering 24, 339–360.

Smith, D.J., Underwood, C., 2000. The production of extracellular carbohydrates by estuarine benthic diatoms: the effect of growth phase and light and dark treatment. Journal of Phycology 36, 321–333.

Smith, D.J., Graham, J., Underwood, C., 1998. Exopolymer production by intertidal epipelic diatoms. Limnology and Oceanography 43 (7), 1578–1591.

Stierle, A., Eicken, H., Krembs, C., Junge, K., Deming, J.W., 2000. Characterization of sedimentary particles and salt precipitates in coastal sea ice from Barrow, Alaska. Abstract, International Symposium on Sea Ice and its Interactions with the Ocean Atmosphere and Biosphere, Fairbanks, Alaska, USA, 19–23 June 2000.

Stoderegger, K., Herndl, G., 1998. Production and release of bacterial capsular material and its subsequent utilization by marine bacterioplankton. Limnology and Oceanography 43, 877–884.

Stoecker, D.K., Gustafson, D.E., Merrell, J.R., Black, M.M.D., Baier, C.T., 1997. Excystment and growth of chrysophytes and dinoflagellates at low temperatures and high salinities in Antarctic sea-ice. Journal of Phycology 33, 585–595.

Sullivan, C.W., Palmisano, A.C., 1984. Sea ice microbial communities: distribution, abundance, and diversity of ice bacteria in McMurdo Sound, Antarctica, in 1980. Applied Environmental Microbiology 47, 788–795.

Sutton, R.L., 1991. Critical cooling rates to avoid ice crystalization in aqueous cryoprotectant solutions containing polymers. Chemical Society Faraday Transactions 87, 3747–3751.

Syvertsen, E.E., 1991. Ice algae in the Barents Sea: types of assemblages, origin, fate and role in the ice-edge phytoplankton bloom. Polar Research 10, 277–287.

Taylor, R., Fletcher, R.L., 1998. Cryopreservation of eukaryotic algae—a review of methodologies. Journal of Applied Phycology 10 (5), 481–501.

Thomas, D.N., Lara, R.J., Eicken, H., Kattner, G., Skoog, A., 1995. Dissolved organic matter in Arctic multi-year sea ice during winter: major components and relationship to ice characteristics. Polar Biology 15, 477–483.

Thomas, D.N., Kattner, G., Engbrodt, R., Giannelli, V., Kennedy, H., Haas, C., Dieckmann, G.S., 2001. Dissolved organic matter in Antarctic sea ice. Annals of Glaciology 33, 297–303.

Underwood, G.J.C., Smith, D.J., 1998. Predicting epipelic diatom exopolymer concentrations in intertidal sediments from sediment chlorophyll *a*. Microbial Ecology 35, 116–125.

UNESCO, 1994. Protocols for the Joint Global Ocean Flux Study (JGOFS) core measurements, IOC Manual and Guides, 29pp.

Weeks, W.F., Ackley, S.F., 1986. The growth, structure and properties of sea ice. In: Untersteiner, N. (Ed.), The Geophysics of Sea Ice. Martinus Nijhoff Publishers, Dordrecht (NATO ASI B146), pp. 9–164.

Weissenberger, J., Dieckmann, G., Gradinger, R., Spindler, M., 1992. Sea ice: a cast technique to examine and analyze brine pockets and channel structure. Limnology and Oceanography 37, 179–183.

Yoshida, H., Hatakeyama, T., Hatakeyama, H., 1990. Phase transitions of the water-xanthan system. Polymer 31, 693–698.

Yoshida, H., Hatakeyama, T., Hatakeyama, H., 1992. Crystallization dynamics of water in polysaccharide hydrogels. In: Maeno, N., Hondoh, T. (Eds.), Physics and Chemistry of Ice. Hokkaido University Press, Sapporo, pp. 284–290.

Zhang, Q., Gradinger, R., Spindler, M., 1998. Dark survival of marine microalgae in the high Arctic (Greenland Sea). Polarforschung 65, 111–116.